

Building Integrated Photovoltaics in Residential Areas:
A Comparative Study of Energy Performance at Different Orientations

*Bygningsintegreerte solcellepanel i boligområder:
En sammenligningsstudie av energipotensial for ulike orienteringer*

Trondheim May 2023

Students:
Hedda Lan Stokke Vøllestad
Ida Bertine Rambøl
Martin Haugen

Internal supervisor:
Bjørn Petter Jelle

External supervisor:
Thomas Engen

Projectnr:
2023 - 35

The report is PUBLIC



Faculty of Engineering

Department of Civil
and Environmental Engineering

Preface

This Bachelor thesis represents the culmination of our three-year bachelor program in building engineering at the Norwegian University of Science and Technology (NTNU). The thesis work is conducted under the supervision of Bjørn Petter Jelle at the Department of Civil and Environmental Engineering.

We thank Bjørn Petter Jelle for his invaluable guidance throughout this research process. His expertise and insights on Building integrated photovoltaics (BIPV), energy performance, and solar radiation harvesting in the Nordic residential area have been instrumental to our understanding of the subject matter. We appreciate Ørland municipality for allowing us to conduct our bachelor's thesis on their project and providing the necessary data and information. We would also like to acknowledge the contributions of Gabriele Lobaccaro, Mattia Manni, Matteo Formolli, and Vegard Andre Skagseth, who offered valuable advice and feedback on the modelling and simulations using Rhino and Grasshopper programs, as well as shared their expertise in the field of solar radiation harvesting and energy performance. Furthermore, we thank Tom Jacobus Franciscus Maria Melkert, Anne Sirnes, and Eskil Walde for their meaningful discussions and collaboration throughout the project.

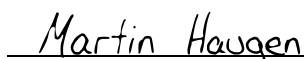
This thesis investigates the possibilities and feasibility of implementing BIPV on listed houses. Our research primarily focuses on a specific project led by Ørland municipality. However, the insights gained from this study can be extrapolated to similar contexts, contributing to a more environmentally friendly future.

The main goal of this research is to evaluate whether BIPV is a viable alternative to building applied photovoltaics (BAPV) despite the higher cost, considering its enhanced durability. Specifically, we aim to advocate for implementing solar panels in the old houses that the Ørland municipality is relocating, feeling the need for facade replacements. Additionally, we aim to investigate the impact of high latitudes on solar power production and address challenges related to strong winds, such as uplift, prevalent in the Ørland region.

After this preface, you will find a table of contents providing an overview of the document's organisation. The introduction section follows, offering a comprehensive outline of the research aims and objectives. Subsequently, the methodology chapter provides detailed explanations of the simulations and procedures employed, allowing readers to replicate the simulations. The results and discussion chapter presents the findings and analysis of our research. Furthermore, the thesis includes a section on different perspectives, where we discuss our visit to a farm in Ørland that has implemented BAPV on two roofs and provide information on its performance during different seasons. Finally, the conclusions and recommendations section summarises the essential findings and offers insights for future actions.

Trondheim 22nd of May 2023.


Hedda L. S. Vøllestad


Martin Haugen


Ida Bertine Rambøl

List of Figures

Fig.1. Listed building - Hoøya 173-34.....	5
Fig.2. Designed model in <i>Rhinoceros 3D</i>	5
Fig.3. The workflow of the simulation, which presents the inputs and the outcome to assess the simulation of the solar accessibility in the municipality of Ørland.....	5
Fig.5. The simulated datapoints, allocated on the corresponding surfaces.	7
Fig.6. The allocation of the building sections, with their assigned colours, dimensioned in cm ²	8
Fig.9. Yearly solar irradiations vs. orientation for the predefined building sections (Fig 6).....	12
Fig.10. Solar irradiations vs. orientation on the building surfaces, during equinoxes and solstices.	14
Fig.11. Total yearly solar irradiation vs. orientation for the entire building envelope.....	17
Fig.12. Solar irradiation falling on the building envelope 0°, the back side of the building facing south. .	18
Fig.13. Optimal orientation maximising the solar irradiation harvesting for the roof and the facade surfaces.	19

List of Tables

Table 1. Main components used to analyse irradiation in <i>Grasshopper</i>	4
Table 2. Simulated analysis periods, grouped in three periodical aspects.	6
Table 3. Estimated area with consideration to the area of windows and doors for every surface.	8
Table 4. Selected BIPV panels and their solar cells electrical efficiency.	8
Table 5. yearly solar energy production considering the most optimal orientation for each of the building surfaces. The calculated solar energy is based on three different efficiencies, which are 18, 16 and 14 percent as listed in Table 4.	16
Table 6. Yearly and seasonal solar energy production by optimising the entire building envelope, given orientation 0 ° and three different solar cells electrical efficiency (Table 4).	19
Table 6. Optimal surfaces combination based on orientation and building section.	20
Table 7. The optimal surface combination to maximise the energy production, for orientation [80°] and [170°].	21
Table 8. The optimal surface combination to maximise the energy production, for orientation [250°] and [360°].	22
Table 9. Summary of the limitations of the conducted methodology and interpretation of this study, presented as advantages and disadvantages.	23

Thesis Contents

Preface	I
List of Figures	III
List of Tables	IV
Thesis Contents.....	V
Building Integrated Photovoltaics: A Seasonal Study of Energy Performance at Different Orientations ...	1
Abstract.....	1
1. Introduction	2
2. Method	4
2.1. Simulation and data collection	4
2.2 Basis for data analysis	7
3. Results and discussion	9
3.1 Numerical approach of the simulations results: comparative interpretation of solar irradiations, considering different simulation periods.....	9
3.1.1 Seasonal approach of harvesting the solar irradiations: comparative interpretation of the four astronomical seasons.....	9
3.1.2 Comparative interpretation of the annual solar irradiation accessibility.....	12
3.1.3 Comparative approach of solar irradiation accessibility during equinoxes and solstices	13
3.2 Optimal orientation for harvesting the solar irradiation	15
3.2.1 Yearly solar energy production considering the most optimal orientation for each of the building surfaces	15
3.2.2 Yearly and seasonal energy production generated from the entire building envelope.....	17
3.3 Optimal combination of the building surfaces: maximisation the energy production, based on orientation and solar irradiation incidence	19
3.3 Limitations of the study	23
4. Conclusion.....	24
Acknowledgements.....	26
References	27
Appendices.....	29
Appendix A – Winter solar energy production	29
Appendix B – Spring solar energy production	30
Appendix C – Summer solar energy production	31
Appendix D - Autumn solar energy production	32

Building Integrated Photovoltaics: A Seasonal Study of Energy Performance at Different Orientations

Ida Bertine Rambøl ^{a#}, Martin Haugen ^{a#*}, Hedda Lan Stokke Vøllestad ^{a#}, Bjørn Petter Jelle ^a,
Gabriele Lobaccaro ^a, Mattia Manni ^a, Matteo Formolli ^b, Vegard Andre Skagseth ^a

^aNorwegian University of Science and Technology (NTNU), Department of Civil and Environmental Engineering, NO-7491 Trondheim, Norway.

^bNorwegian University of Science and Technology (NTNU), Department of Architecture and Technology, NO-7491 Trondheim, Norway.

[#]These authors have contributed equally.

* Corresponding author: haugenmartin91@gmail.com

Abstract

The conducted study evaluates the variation of the solar irradiation accessibility in a consolidated Nordic built environment. The approach is applied to a case study located at the municipality of Ørland, Norway; latitude 63.7828° N. The objective is to examine the possibility of installing building integrated photovoltaics (BIPV) on one of the relocated cultural heritage houses, as well as analyse the solar irradiation accessibility on the building envelope. A series of solar simulations are conducted to determine the solar irradiation accessibility during different periods, using climate data as basis metric. The results show the variation of the solar accessibility between the astronomical seasons, and the annual irradiation incidence, on the building surfaces. In this context, the solar irradiations accessibility during winter and autumn are drastically lower than those during spring and summer, which negatively affect the energy production during those seasons. Furthermore, the simulation results indicate that the most optimal orientation for each of the building surfaces varies significantly according to the simulation periods. Hereby, the energy production can be maximised by finding the optimal orientation for each of the surfaces and subsequently determining the most optimal surfaces combination for BIPV panels installation. The findings from the conducted analyses, show that roof tiles BIPV installation would be optimal for annual energy production, while the BIPV panels installation on selected facade surfaces would maximise the energy production during the critical seasons, i.e. winter and autumn. Moreover, the calculated results for the total energy production, shows that covering the dwelling entire energy consumption is very challenging. This study demonstrates how the solar incidence varies correspondingly to the simulation period, and how this can affect the energy production.

Keywords:

Building integrated photovoltaic, energy efficiency, cultural heritage law, listed buildings, cultural heritage law, simulation, sustainable energy, environmental analysis, solar incidence, irradiation accessibility, harvesting solar irradiation, energy consumption.

Acronyms

BIPV	Building integrated photovoltaic
PV	Photovoltaic
POA	Plane of array [kWh/m ²]
Irr	Solar Irradiation

1. Introduction

As the world embraces sustainable practices and seeks to transition towards a greener future, the increased adoption of solar power plays a pivotal role in driving the green revolution. Solar energy offers immense potential for meeting rising electricity demands while mitigating carbon emissions [1,2]. Building integrated photovoltaics (BIPV) greatly contributes to the building industry's sustainability and shows a consistent development in both efficiency and architectural appearance [3,4]. In Norway, solar power is gaining popularity, and advancements in technology continue to enhance the effectiveness of solar panels [5–7].

Situated in central Norway along the Trondheim Fjord, latitude 63.7828° N, Brekstad is undergoing a transformation of relocating 22 listed houses, from areas affected by noise pollution from a nearby military air force base. Complementing this effort, 33 new homes will be constructed in harmony with the scale and placement of the historic buildings, forming a new residential area at Brekstadbukta. In conjunction with this project, the municipality of Ørland aims to explore the feasibility of implementing BIPV systems in the old and new houses, while still maintaining the considerations of the local cultural heritage law [8].

Brekstad presents a unique setting characterised by flat lands and strong winds, occasionally accompanied by storms and hurricanes [9]. These prevailing winds pose challenges to the secure installation of solar panels, potentially causing uplift and structural instability [10]. Considering these factors, BIPV emerges as a promising solution that seamlessly blends with the architectural style of existing structures, providing enhanced stability. A sturdier structure is necessary to secure against uplift, but BIPV eliminates this requirement by leaving no room between the panels and the facade. This feature avoids the cost, embodied energy, and corresponding emissions associated with structural units, making the marginal material cost much lower than retrofitting photovoltaics (PV) into a typical system [11].

The geographical location of Brekstadbukta offers a moderate amount of sun hours during the summer months but experiences limited sun exposure during the winter. Considering the winter solstice, the region sees only 4 hours of sunlight during the day, with a maximum altitude of 2.8°. However, Brekstad has over 20 hours of daylight during the summer solstice, with the sun reaching almost 48° [12]. By strategically incorporating solar panels on building facades and rooftops, there is a tremendous opportunity to harness and maximise sunlight during the darker winter months. This approach ensures that solar panels capture optimal solar radiation, regardless of the challenging conditions of low winter sun angles. It is also possible to combine BIPV with other technologies to improve efficiency in harsh weather conditions. An example of this can be reuse of heat by air source heat pump [13], or avoiding snow and ice formation using repellent, superhydrophobic and icephobic surfaces [14].

The physics behind solar irradiation is non-trivial; therefore, software such as *Rhinoceros 3D* and *Grasshopper* can be beneficial in analysing the realistic potential for energy production [15]. The structure of these programmes facilitates customisation of the simulation to suit specific circumstances with a wide selection of plug-ins and components [16–19]. This study's analysis primarily relies on a simulation using *Ladybug*, *Radiance Tool* and *Colibri* plug-ins. These makes it easier to calculate the irradiance on building surfaces, divided into different sections, for several orientations and analysis periods.

In summary, the objective of this study is to investigate the viability of building integrated photovoltaics for solar power generation in the challenging environment of Brekstad, Norway. By addressing wind conditions, architectural considerations, and seasonal variations in sunlight availability, this research aims to provide practical knowledge and support decision-making for successfully implementing BIPV systems in similar contexts. Adopting BIPV can promote sustainable energy practices and contribute to a greener future for communities facing similar challenges.

2. Method

2.1. Simulation and data collection

To assess the potential energy production of BIPV implementation on listed buildings in a high-latitude area, this study aims to evaluate the associated obstacles. To gain an understanding of the possibilities and challenges surrounding this, inspections of the buildings and the local area were conducted. Based on these observations, data was collected using a simulation performed in the CAD 3D modelling software *Rhinoceros 3D* and the parametric modelling tool *Grasshopper* [15]. Various components from the plugins *Ladybug* and *Radiance Tool* were utilised to analyse the irradiation further. As well as components from *Colibri* that automate the simulation with a wider range of iterations. The main components from the simulation are summarised in Table 1.

Table 1. Main components used to analyse irradiation in *Grasshopper*.

Section	Subsections	Components
First Section	Climate Data	LB Download Weather
		LB Import EPW
	Analysis Period	LB Analysis Period
	Orientation	Number slider
Second Section	Sky Matrix	LB Cumulative Sky Matrix
Third Section	Building Geometry	Geometry
	Incident Radiation	LB Incident Radiation Point List
Fourth Section	Subset	Sub List
	Colibri Automation	Colibri Inputs
		Colibri Outputs Colibri Aggregator
Extra	Visualise Sun Path	LB Sun Path
		LB Sky Dome
	Area of Geometry	Area

The model used in the simulation represents a listed building that reflects the general architectural style of the residential area. It was modelled in *Rhinoceros 3D* based on estimated measurements from one of the existing buildings that are being relocated, as presented in Fig1 and 2. This building showcases numerous projections extending in various directions, along with two chimneys that cast shadows influencing the potential energy generation in distinct manners depending on their orientations. Additionally, it encompasses two distinct roof inclinations, approximately at 45° and 30°.



Fig.1. Listed building - Hoøya 173-34

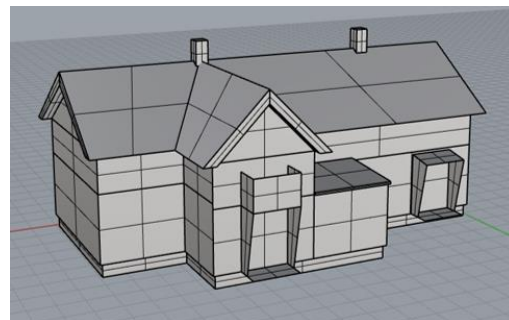


Fig.2. Designed model in *Rhinoceros 3D*

Due to the building's asymmetry and the high variation of radiation and sun hours, it was essential to simulate all possible orientations and seasons for a holistic evaluation of energy production potential. This simulation can be divided into four sections, as illustrated by the colours in Fig.3 below.

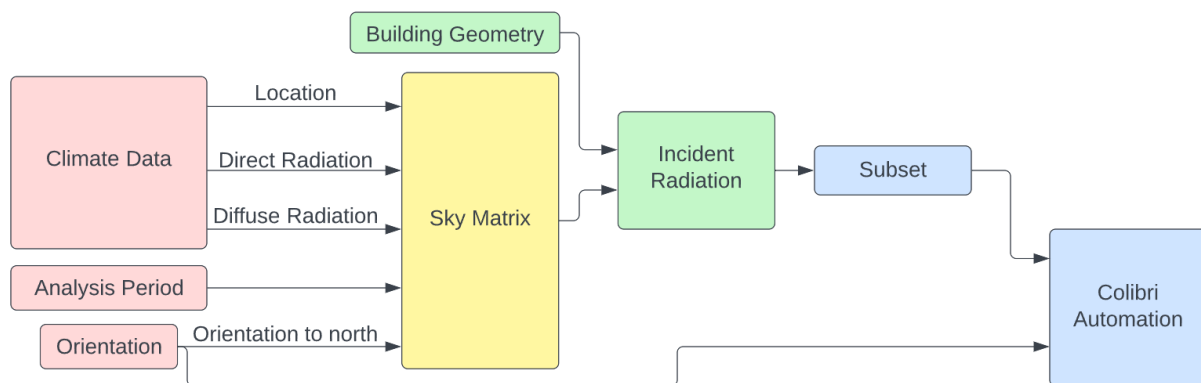


Fig.3. The workflow of the simulation, which presents the inputs and the outcome to assess the simulation of the solar accessibility in the municipality of Ørland.

The first section includes the primary input data for climate, analysis period, and orientation. For climate data, the simulation uses a dataset sourced from *Climate One Buildings*, which comprises a 15-year dataset from 2007 to 2021 in Ørland [20]. A *Grasshopper* slider was connected to the *north* input in the *LB Cumulative Sky Matrix* to collect data for a range of orientations. This rotates the sun path counter-clockwise by 10° increments, ranging from 0° to 360°, as shown in Fig.4, where the path starts with south facing the back side of the building at 0°. To differentiate the simulated data, the simulation is conducted nine times with varying analysis periods for each run-through, as detailed in Table 2.

Table 2. Simulated analysis periods, grouped in three periodical aspects.

Analysis Period		Dates
Yearly	Year	1. Jan. to 31. Des.
Seasons	Autumn	23. Sept. to 21. Des.
	Winter	22. Des. to 19. March
	Spring	20. March to 20. June
	Summer	21. June to 22. Sept.
Equinox and Solstice	Autumn Equinox	23. Sept.
	Winter Solstice	22. Des.
	Spring Equinox	20. March
	Summer Solstice	21. June

* Based on an average of a dataset over the span of 15 years

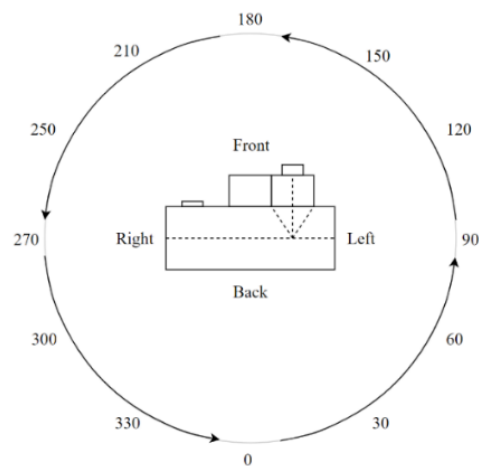


Fig.4. Orientation of sun path starting at 0°, with the back side of the building facing south.

The second section is the sky matrix, which uses the data from the first section to create a matrix containing radiation values from each patch of a sky dome. This matrix can be visualised in *Rhinoceros 3D* as a sun path and a sky dome, making it easy to troubleshoot and debug the input data collected in section one. The sky matrix connects to the component *LB Incident Radiation* in section three. This, along with selected geometry and context, creates a list of irradiation results for a chosen grid size. In this case, the number of results was minimised by selecting parts of the building as context instead of geometry. All data points in the chosen grid are visualised on the model using the component *Point list*; in this case, there are 96 data points, as illustrated in Fig 5.

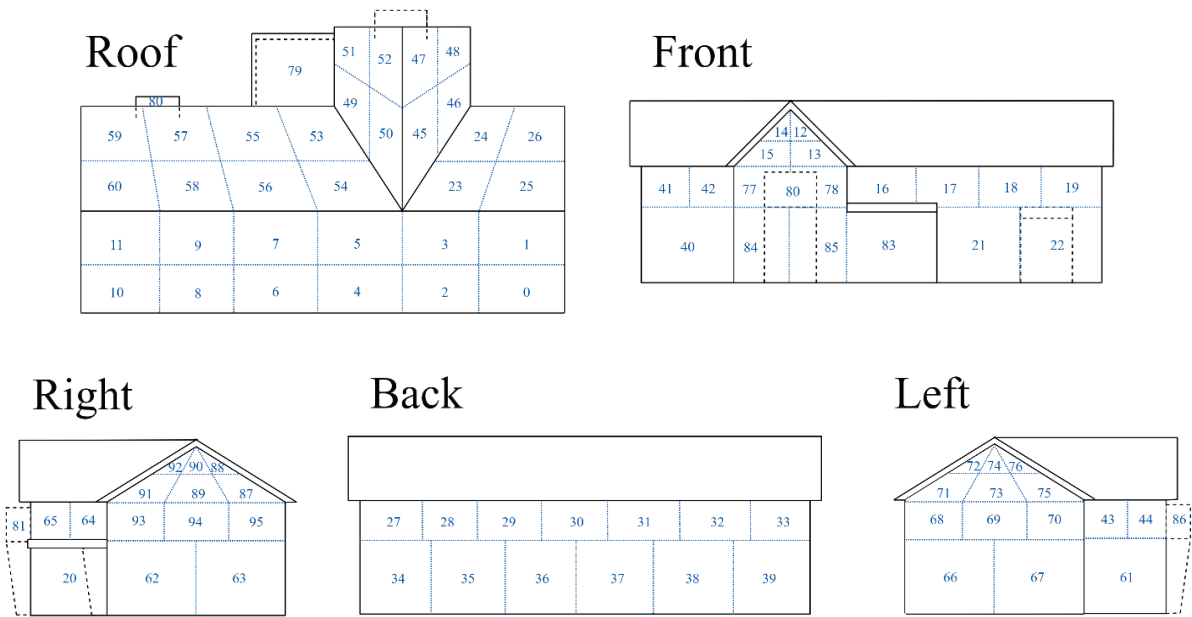


Fig.5. The simulated datapoints, allocated on the corresponding surfaces.

In the last section the *Colibri* components iterate through all combinations for a series of orientations and analysis periods and compile the results into a CSV-file. The *Colibri Output* component that collects the results is limited to ten values max for each grip. Since the model is divided into 96 data points, it is necessary to split these into subsets of ten each.

2.2 Basis for data analysis

The 96 datapoints conducted from the simulation are decreased into 18 different surfaces, see Fig.6, to make a facilitated distinction when analysing the simulated data. These surfaces were carefully selected based on the average solar irradiation of the datapoints that represent each of the surfaces. In Fig. 6 the surfaces are visualised in four segments with a variation of colours assigned, these segments are later used to visualise the simulated results, in the result and discussion section. The dimensions of these surfaces are based on provided measurements, as well as some assumptions based on standardized measurement. Table 3 gives the estimated net area calculated to conduct this study, with consideration to window and door surfaces.

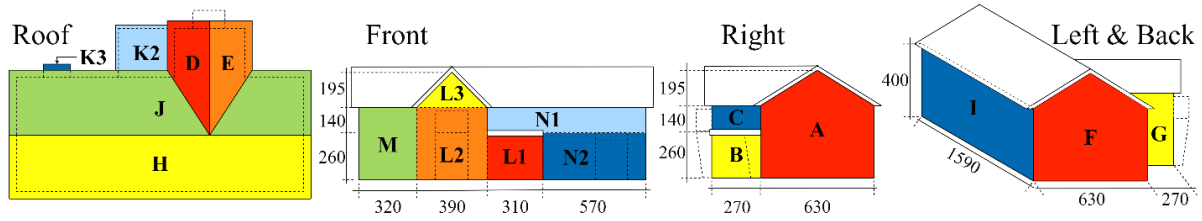


Fig.6. The allocation of the building sections, with their assigned colours, dimensioned in cm2.

Table 3. Estimated area with consideration to the area of windows and doors for every surface.

	A	B	C	D	E	F	G	H	I	J	K1	K2	K3	L1	L2	L3	M	N1	N2
Area [m ²]	31.3	6.6	3.8	15.3	15.3	28.5	10.8	73.4	47.4	62.6	4.6	8.8	1.8	7.4	12.4	3.2	12.6	8.0	11.4

Different types of solar cell modules have different electrical efficiencies according to the manufactured material and colour [21]. The energy production for each surface is obtained by multiplying the solar irradiation by the efficiency, as presented in Eq. 1. Hence, this variation in the solar cell efficiency affects the energy production. Table 4 show a list of the BIPV panels, selected for this case study, and their solar cells electrical efficiency.

$$Energy \left[\frac{kWh}{t} \right] = Irradiation \left[\frac{kWh}{m^2 \cdot t} \right] \cdot Area [m^2] \cdot Efficiency [\%] \quad (1)$$

* t = simulated analysis period

Table 4. Selected BIPV panels and their solar cells electrical efficiency

Number	Efficiency [%] *	Building section
1	18	Roof and facade
2	16	Roof and facade
3	14	Roof and facade
4	18	Roof Shingle
5	11	Facade

* Module efficiency values provided by sample supplier.

3. Results and discussion

In this section, the main findings from the conducted simulations are presented according to three interdependent sections, followed by a presentation of the limitation of this study. The first section is a numerical approach of the simulation results, which focuses on a comparative interpretation of different simulation periods, in terms of solar irradiation accessibility. The second section focuses on determining the most optimal orientation for harvesting the solar irradiation, based on the output from the simulation results. Finally, the third section focuses on finding the most optimal combination of the predefined building surfaces maximising the energy production.

3.1 Numerical approach of the simulations results: comparative interpretation of solar irradiations, considering different simulation periods

The simulation results for the global solar irradiation, provide numerical values of the solar irradiation accessibility, for the different building surfaces. This numerical approach focuses on the solar irradiation performance throughout the four astronomical seasons, annual harvesting of solar irradiation, and a comparative approach of the solar irradiation accessibility during equinoxes and solstices (Table 2) The results of the conducted simulation are computed based on a range of orientations between 0° to 360°, by 10° increments (Fig 7, 8, 9, and 10). Such solar irradiation values are used as bases to determine the variation of solar incidence on the different building sections, for each of the simulation periods, as well as the effect of the building orientation on harvesting the solar irradiation. These bases are used later as an input to calculate the energy production obtained from each of the building surfaces at their optimal orientation, as well as to facilitate the determination of the best possible combination of building surfaces, maximising the energy production.

3.1.1 Seasonal approach of harvesting the solar irradiations: comparative interpretation of the four astronomical seasons

The simulation results, for the four astronomical seasons, are presented in Fig.7 and Fig 8, where the seasonal values of solar irradiations are graphically represented. Fig. 7, consists of 4 different series of graphs, where each series shows the numerical values of the solar irradiations on the predefined building sections. On the other hand, Fig.8, shows the seasonal difference in the amount of the solar irradiation received by the entire building envelope, for each orientation.

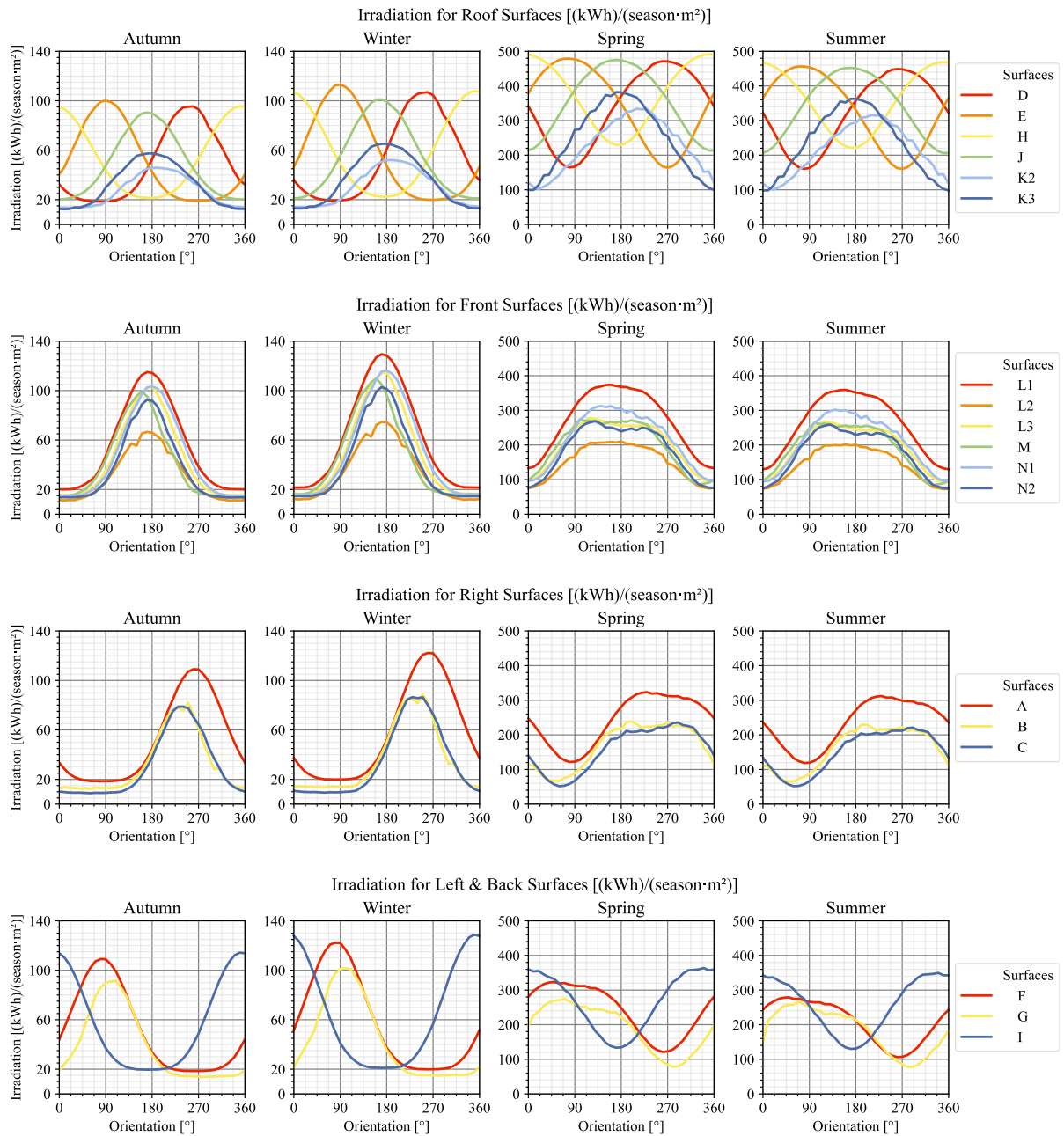


Fig.7. Solar irradiation vs orientations throughout the astronomical seasons for each of the predefined building surfaces (Fig 6).

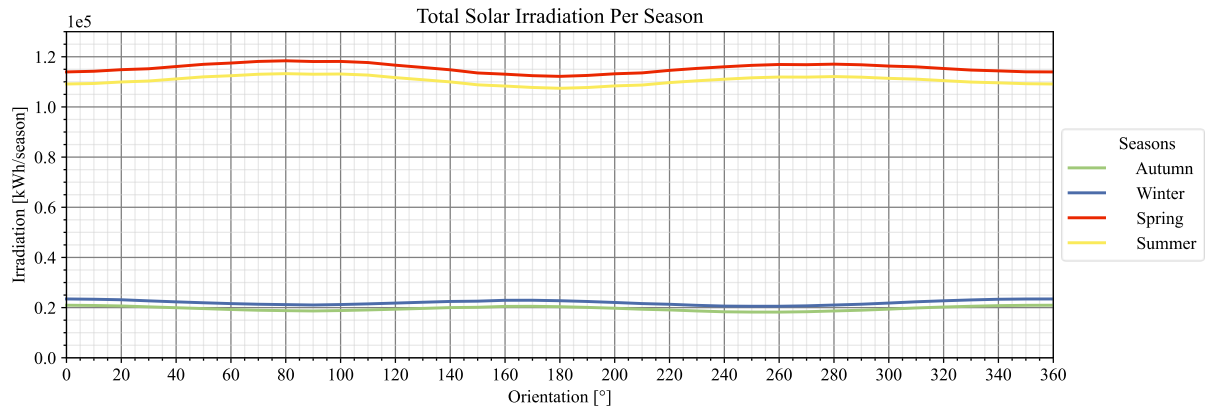


Fig.8. Total solar irradiation vs. orientations per season for the entire building envelope.

Several observations can be made, when interpreting the graphs listed in Fig. 7 and 8. Firstly, the values of the solar irradiation are slightly higher in winter than autumn, and higher in spring than summer. This could be related to the differing sun position from one season to another; in the northern hemisphere the sun moves northward across the celestial equator during spring and summer, and southward during autumn and winter [16]. Moreover, the differing sun hours throughout the seasons and the reduction of the plan of array (POA) irradiance during November and December, cause a reduction in the average solar irradiation during autumn [22]. Another observation is that the roof surfaces H, E, J, and D, receive, at their optimal orientation, higher solar irradiation than the rest of the building surfaces during spring and summer. In fact, the predefined roof surface H receives the highest solar irradiation among all the building surfaces, with an $Irr=491.5$ [kWh/ (m² spring)] and $Irr=468.45$ [kWh/ (m² summer)]. Finally, the facade surfaces L1, I, A, F, N1 and L3, receive slightly higher irradiation, during winter and autumn, than any of the roof surfaces. Therefore, considering this could be valuable to optimise the energy production during winter and autumn, since these seasons are the most critical for energy production, due to the (i) low amount of sun hours during winter and autumn, (ii) climate affect, such as wind and heavy clouds, (iii) reduction of the POA due to snow accumulation on the roof surfaces [22]. Hence, based on these results, the facade surfaces are the most optimal for BIPV installation, during winter and autumn. More findings about the optimal orientation, for each of the building surfaces, and maximisation the solar energy production is described in details in section 3.2.

3.1.2 Comparative interpretation of the annual solar irradiation accessibility

The Numerical values for the annual solar irradiation incidence, falling on the predefined building sections, are graphically represented in Fig.9. These graphs display the variation in solar irradiations performance for each of the building surfaces, considering different orientations.

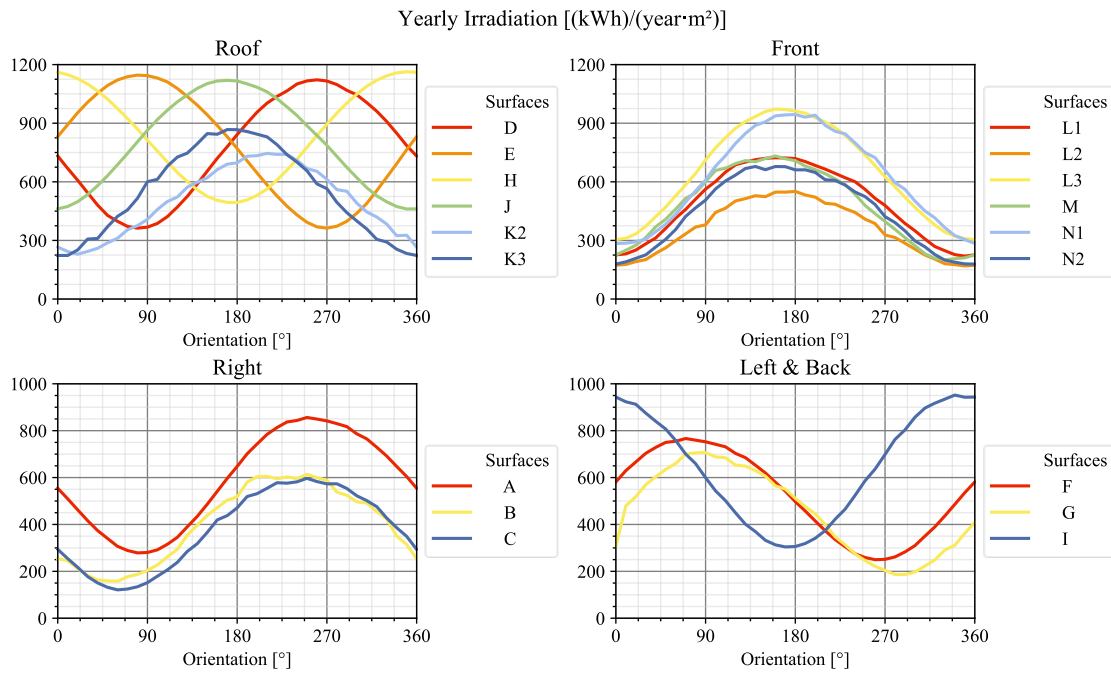


Fig.9. Yearly solar irradiations vs. orientation for the predefined building sections (Fig 6).

The outcome of the yearly solar irradiation, presented in Fig. 9, leads to several findings. Firstly, the solar irradiations falling on the roof surfaces H, E, J and D, at their optimal orientation, are relatively higher than the rest of the building surfaces. This could be due to the fact that the predefined roof slopes (45 and 30°) increase the penetration of the POA irradiance on the roof surfaces throughout the year. Comparatively, the roof surfaces receive relatively higher solar irradiation during spring and summer, which increase the solar irradiation accessibility on these surfaces throughout the year. Another finding is that the facade surface L3 receives the highest solar irradiation among the facade surfaces. However, L3 is not necessarily the most optimal surface for energy production due to its relatively smaller area compared to surfaces such as I, A and F. Moreover, it is very challenging to optimise the entire surface area due to windows installation. Comparatively, the surfaces I, A and F have a bigger area and a relatively high perception of solar irradiations, making them the most optimal surfaces for BIPV installation and

for optimising the energy production throughout the year. Finally, maximising the yearly energy production depends on finding the most optimal surfaces in terms of area, as well as the surfaces accessibility to the annual solar irradiation.

3.1.3 Comparative approach of solar irradiation accessibility during equinoxes and solstices

The different solar irradiation accessibility during spring and autumn equinoxes, as well as winter and summer solstices, are graphically represented in Fig.10. The simulation results during these days are presented in four series of graphs, where each series represents the values of the solar irradiation accessibility for the predefined building sections.

The plotted values of the solar irradiation accessibility during equinoxes and solstices, Fig.10, leads to several observations. One of the observations is that the summer solstice, as well as the autumn and spring equinoxes, can, to some extent, represent the solar irradiation of their corresponding astronomical season. In fact, there is a strong similarity when comparing the shape of the curves for these three days (Fig.9) with their corresponding seasons (Fig.7). However, the results show that the solar irradiation for the winter solstice is almost equal to 0, meaning that this day could not be a good representative for the solar incidence during winter. Another observation is that the spring equinox is overall characterized by higher solar irradiations than the autumn equinox. This could be also related to the fact that the spring equinox occurs when the sun moves northward across the celestial equator, while the autumn equinox occurs when the sun crosses the celestial equator, going southward [16]. Finally, the summer solstice is not a good representative of the most optimal energy production that could be obtained in one day. This could be due to the climate data during the simulated period [simulation climate data for Ørland], such as weather conditions, heavy cloud, or rain, as well as the high temperatures hitting the solar panels, which can affect their thermal efficiency [23].

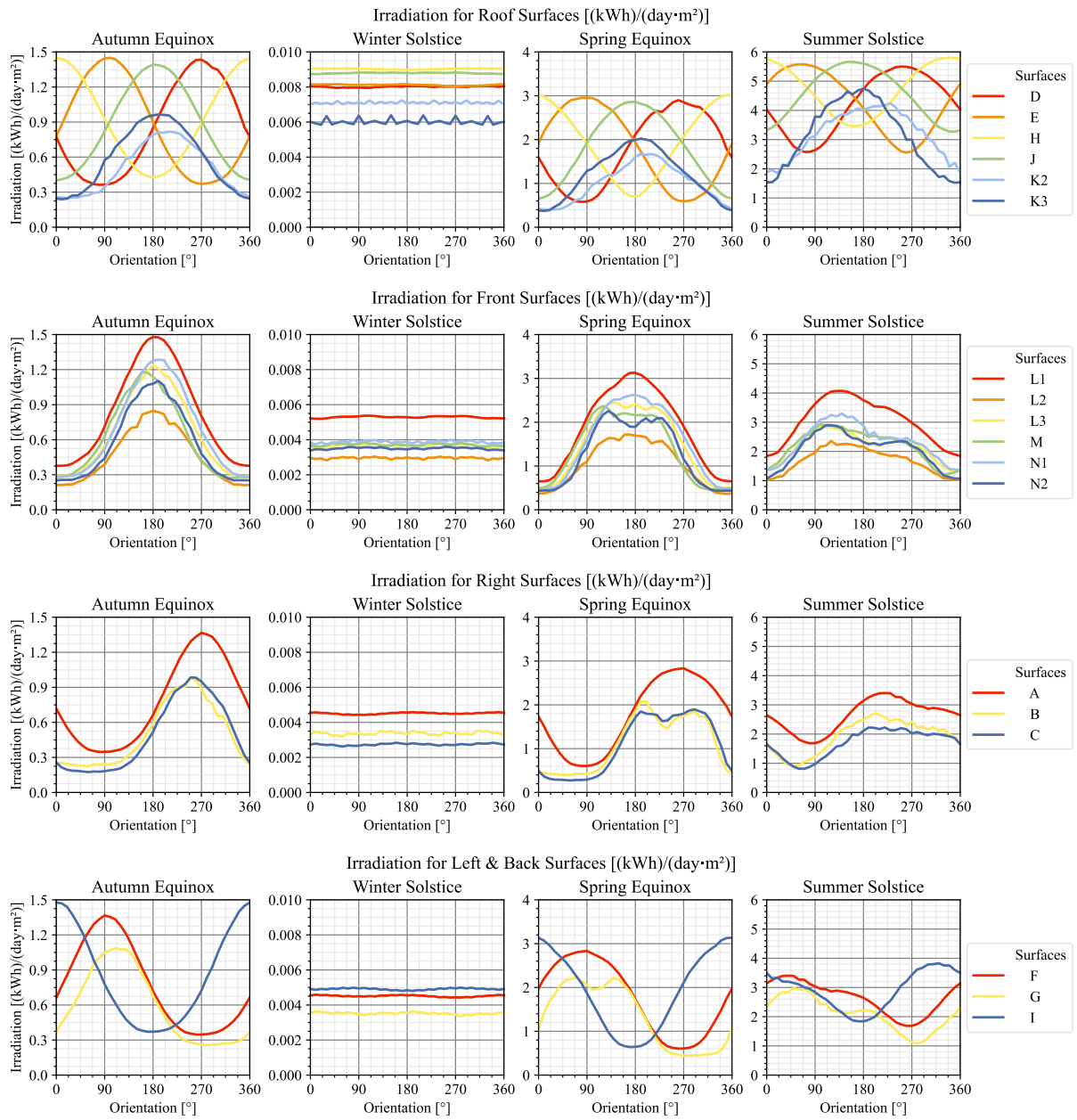


Fig.10. Solar irradiancies vs. orientation on the building surfaces, during equinoxes and solstices.

3.2 Optimal orientation for harvesting the solar irradiation

3.2.1 Yearly solar energy production considering the most optimal orientation for each of the building surfaces

The results output from the conducted yearly simulation are used as an input in Table 5. The optimisation performed on the simulated data demonstrates which orientation is the most optimal for the annual energy production, for each of the building surfaces. In practice, the solar incidence on the different building surfaces varies drastically by changing the orientation of the building. Therefore, harvesting the highest possible solar energy requires to determine the most optimal orientation of the building surfaces, based on the solar irradiation accessibility. It is also important to observe that, the optimal orientation varies according to the simulation period. This variation could be observed in the listed graphs in Fig.7 and the calculated data presented in Table 5. More calculations for the energy production and the variation of the optimal orientation throughout the seasons are presented in Appendix A, B, C and D.

Table 5. yearly solar energy production considering the most optimal orientation for each of the building surfaces. The calculated solar energy is based on three different efficiencies, which are 18, 16 and 14 percent as listed in Table 4.

		Yearly					
Surfaces	Optimal Orientation	Solar Irradiation			Solar Energy [kWh/t*area]		
		[°]	[kWh/m ² *t]	[kWh/A*t]	Efficiency		
					18 %	16%	14%
Right Facade	A	250	856.30	26838.70	4830.97	4294.19	3757.42
	B	250	613.77	4044.74	728.05	647.16	566.26
	C	250	596.69	2255.51	405.99	360.88	315.77
Left & Back Facade	F	70	856.30	24372.54	4387.06	3899.61	3412.16
	G	70	708.12	7647.70	1376.59	1223.63	1070.68
	I	340	951.84	45117.04	8121.07	7218.73	6316.39
Front Facade	L1	160	972.40	7234.68	1302.24	1157.55	1012.86
	L2	180	550.78	6829.69	1229.34	1092.75	956.16
	L3	160	723.25	2316.22	416.92	370.60	324.27
	M	160	732.25	9189.71	1654.15	1470.35	1286.56
	N1	160	819.73	6557.84	1180.41	1049.25	918.10
	N2	140	678.45	7720.75	1389.74	1235.32	1080.91
Roof	D	260	1122.05	17203.05	3096.55	2752.49	2408.43
	E	80	1146.23	17573.87	3163.30	2811.82	2460.34
	H	350	1163.25	85398.28	15371.69	13663.73	11955.76
	J	170	1135.44	71127.60	12802.97	11380.42	9957.86
	K2	210	745.63	6593.23	1186.78	1054.92	923.05
	K3	170	867.37	1592.18	286.59	254.75	222.91

t= simulation period (year), *A*= surface area

The calculated results in Table 5, shows that the energy production varies drastically according to the solar cells electrical efficiency. Therefore, it is possible to demonstrate that installing BIPV system with high efficiency, considering the Nordic climate, has certain advantages. These advantages are ranging from that the solar cells with high efficiency are optimal due to the low temperature during late autumn and winter, as well as the moderate temperature during summer and spring [23]. In addition, the significant amount of annual sun hours, at the Nordic regions is higher than in others locations in central Europe [22].

Moreover, these advantages are ranging from the higher solar energy potentiality on vertical surfaces, i.e. facade surfaces, due to the low angle of solar rays during autumn and winter, which could make it optimal to increase the energy production during winter and autumn. Finally, interpreting the calculated data Table 5, shows that solar irradiation performance varies between the building surfaces. Herby, the roof surfaces H and J are the most optimal to maximise the energy production due to their high solar irradiation performance, and to their relatively big surface area.

3.2.2 Yearly and seasonal energy production generated from the entire building envelope

The results from the annual (Fig.11) and seasonal (Fig.7) conducted simulations, give the total solar irradiation accessibility for the entire building envelope, considering all the simulated orientations. However, determining the overall optimal orientation for harvesting the solar irradiation, is challenging considering that each simulation period has a different optimal orientation. Therefore, the optimal orientation for the building envelope should preferably be determined based on the highest solar irradiation accessibility during winter and autumn, considering these seasons are the most critical for energy production. In this context, orienting the building envelope at 0° (back side of the building facing south, see Fig.12, would be the most optimal for maximising the energy production.

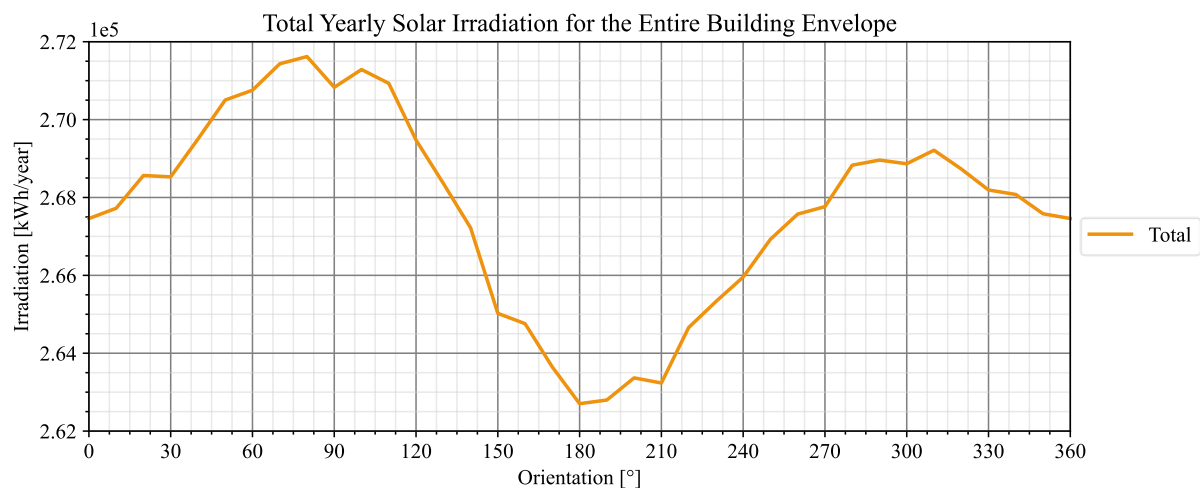


Fig.11. Total yearly solar irradiation vs. orientation for the entire building envelope

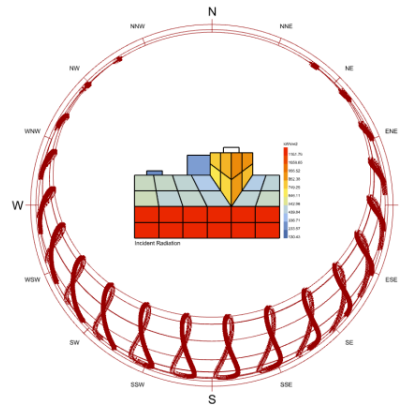


Fig.12. Solar irradiation falling on the building envelope 0° , the back side of the building facing south.

The potential energy production can be obtained by multiplying the solar irradiation on the building envelope (oriented at 0°), with the solar cells electrical efficiencies (Eq. (1)). However, determining the covered energy consumption based on the harvested solar energy, varies according to the electricity usage, measured building area, location, and dwelling condition. The estimated energy consumption for a residential house in Norway lays within an interval of 15500 – 17500 [kWh/year] [24]. Based on this estimation and considering that the minimum yearly harvested solar energy on the building envelope is 37444.3 kWh/year (Table 6), the entire electricity usage for a residential dwelling in the municipality of Ørland can be largely covered. On the other hand, it is very challenging to estimate the seasonal energy consumption due to drastic variations in consumption between seasons. Indeed, in Nordic regions, the electricity usage is much higher in winter and autumn, than spring and summer. Therefore, it is difficult to assess whether the harvested energy would cover the energy requirements during winter and autumn, due to the higher energy consumption and the impracticability to store the harvested solar energy in batteries over a long period of time.

Table 6. Yearly and seasonal solar energy production by optimising the entire building envelope, given orientation 0 ° and three different solar cells electrical efficiency (Table 4).

Period	Solar irradiation Accessibility [kWh/A .t] *	Energy production [kWh/A.t] *		
		Given Efficiency [%]		
		18	16	14
Yearly	267459.2	48142.7	42793.5	37444.3
Winter	23449.7	4220.9	3752.0	3283.0
Spring	113953.2	20511.6	18232.5	15953.4
Summer	109137.0	19644.7	17461.9	15279.2
Autumn	20953.1	3771.6	3352.5	2933.4

*A= Building envelop area, t= simulation period

3.3 Optimal combination of the building surfaces: maximisation the energy production, based on orientation and solar irradiation incidence

The results output from the conducted simulation, are used as in input in Table 6, 7 and 8, to determine the best possible combination of the building surface, maximising the energy production. Each of these combinations is selected by interpreting the different orientations of the building envelope, and assessing the highest solar irradiation accessibility at specific orientations. Based on this interpretation, orienting the building at 80, 170, 250 and 360°, see Fig.13, will allow the building surfaces (defined in Fig.6) to receive the highest possible solar irradiation, maximising the energy production. In this context, the combinations are presented respectively for the facade and the roof in Table 6.

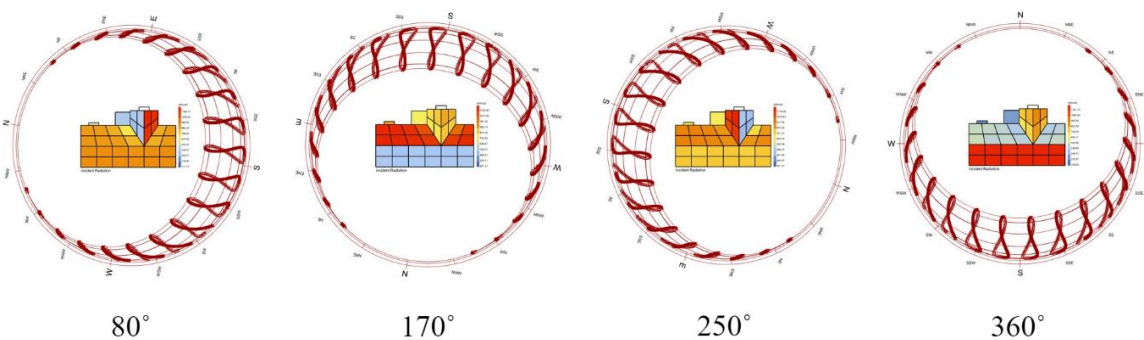


Fig.13. Optimal orientation maximising the solar irradiation harvesting for the roof and the facade surfaces.

Table 6. Optimal surfaces combination based on orientation and building section.

Orientation [°]	Building section facing south	Optimal combinations	
		Roof	Facade
80	Right	E, H & J	F, G, I and M
170	Front	J, E, D & K2	L3, N1, L1, M
250	Left	D, J, H & K2	A, B, C, & L1
360	Back	D, E, H & J	I, F, A & G

The optimal building surfaces combination (defined in Table 6), facilitate maximising the energy production from the BIPV panels, on the roof and facade surfaces. The cultural heritage demands in Norway, make some limitation in selecting the colour and the type of the BIPV panels. In this context, taking into consideration that the simulated module represents a cultural heritage dwelling in the municipality of Ørland, the reliable BIPV panel would be a black BIPV Solar Tile Shingles, with an electrical efficiency of 18%, for the roof surfaces, and a white BIPV solar panels, with an electrical efficiency of 11%, for the facade surfaces, (Table 4). Table 7 and 8, show the average yearly and seasonal solar irradiation per m², the total solar irradiation per combination area, the average energy production per m² per combination, and the total energy production by each of these combinations.

Table 7. The optimal surface combination to maximise the energy production, for orientation [80°] and [170°].

			Optimal Combinations					
			[80°]			[170°]		
			Roof	Facade	Overall	Roof	Facade	Overall
Year	Irradiation	[kWh/m ² .t]	940.3	666.9		855.0	838.2	
		[kWh/A.t]	131848.9	67306.9	199155.8	100918.0	25031.0	125949.1
	Energy	[kWh/m ² .t]	169.3	73.4		153.91	92.20	
		[kWh/A.t]	23732.8	7403.8	31136.6	18165.25	2753.41	20918.66
Winter	Irradiation	[kWh/m ² .t]	72.2	78.1		64.7	115.9	
		[kWh/A.t]	8862.4	7459.5	16321.9	8423.6	3569.2	11992.8
	Energy	[kWh/m ² .t]	13.0	8.6		11.65	12.75	
		[kWh/A.t]	1595.2	820.5	2415.8	1516.25	392.61	1908.86
Spring	Irradiation	[kWh/m ² .t]	412.1	277.2		374.8	284.9	
		[kWh/A.t]	59011.7	28549.9	87561.7	43479.5	8873.3	52352.8
	Energy	[kWh/m ² .t]	74.2	30.5		67.47	31.33	
		[kWh/A.t]	10622.1	3140.5	13762.6	7826.30	976.07	8802.37
Summer	Irradiation	[kWh/m ² .t]	393.0	257.8		357.8	287.6	
		[kWh/A.t]	56276.3	26341.3	82617.6	41451.1	8965.4	50416.5
	Energy	[kWh/m ² .t]	70.7	28.4		64.41	31.64	
		[kWh/A.t]	10129.7	2897.5	13027.3	7461.20	986.19	8447.39
Autumn	Irradiation	[kWh/m ² .t]	63.5	69.0		57.5	103.7	
		[kWh/A.t]	7783.5	6629.4	14412.9	7516.7	3198.9	10715.6
	Energy	[kWh/m ² .t]	11.4	7.6		10.35	11.41	
		[kWh/A.t]	1401.0	729.2	2130.3	1353.01	351.88	1704.88

*A= Building envelop area, t= simulation period

Table 8. The optimal surface combination to maximise the energy production, for orientation [250°] and [360°].

		Optimal Combinations					
		[250 °]			[360 °]		
		Roof	Facade	Overall	Roof	Facade	Overall
Year	Irradiation	[kWh/m ² .t]	862.08	657.02		796.42	596.48
		[kWh/A.t]	135611.42	37315.08	172926.50	138090.6	819467.0
	Energy	[kWh/m ² .t]	155.17	72.27		143.4	65.6
		[kWh/A.t]	24410.06	4104.66	28514.72	24856.3	9014.2
Winter	Irradiation	[kWh/m ² .t]	61.88	89.68		52.71	59.57
		[kWh/A.t]	8732.12	5163.82	13895.94	10457.4	8928.6
	Energy	[kWh/m ² .t]	11.14	9.87		9.5	6.6
		[kWh/A.t]	1571.78	568.02	2139.80	1882.3	982.1
Spring	Irradiation	[kWh/m ² .t]	380.78	271.61		356.30	271.54
		[kWh/A.t]	60759.37	14738.89	75498.26	60475.3	34932.3
	Energy	[kWh/m ² .t]	68.54	29.88		64.1	29.9
		[kWh/A.t]	10936.69	1621.28	12557.96	10885.6	3842.5
Summer	Irradiation	[kWh/m ² .t]	362.88	259.42		340.38	250.97
		[kWh/A.t]	58011.97	14124.53	72136.50	57790.5	32521.2
	Energy	[kWh/m ² .t]	65.32	28.54		61.3	27.6
		[kWh/A.t]	10442.16	1553.70	11995.85	10402.3	3577.3
Autumn	Irradiation	[kWh/m ² .t]	55.85	80.64		47.06	52.60
		[kWh/A.t]	7922.80	4609.10	12531.90	9373.0	7906.3
	Energy	[kWh/m ² .t]	10.05	8.87		8.5	5.8
		[kWh/A.t]	1426.10	507.00	1933.11	1687.1	869.7

*A= Building envelop area, t= simulation period

The calculated results for each of the combination in Table 7 and 8, give a good estimation of a yearly energy production, for each of the selected combination of surfaces, and show how harvesting the solar energy varies drastically throughout the seasons. These results shows that the energy production during spring and summer is approximately 4 to 5 times higher than the energy production during winter and autumn. Moreover, it is very challenging to cover the entire energy requirement for a residential house during winter and autumn, due to the high energy consumption and the low energy production during these seasons. Therefore, covering the entire energy consumption during winter and autumn, requires increasing the installation area of the BIPV panels, as well as chose the most optimal electrical efficiency commercially available. Finally, the reduction of the plan of array due to the snow accumulation on the roof surfaces, affects the energy production during the snow periods.

Thereby, to optimise the energy production during the snow period, there are two essential parameters that should be taken into consideration: (i) techniques for snow removal should be implemented to boost solar energy penetration at high latitudes [22], and (ii) rely mostly on the facade surfaces to optimise the energy production during winter and autumn.

3.3 Limitations of the study

In this section, the limitations of the study are presented. A summary of these is provided in table 9, where the advantages and limitations of the methodology are presented.

Table 9. Summary of the limitations of the conducted methodology and interpretation of this study, presented as advantages and disadvantages.

Topic	Advantages	Disadvantages
Shadowing from the surrounding buildings is not accounted for	<ul style="list-style-type: none"> • Increase harvesting the solar irradiation • Increase the potentiality for BIPV installation • Resulting in higher energy production 	<ul style="list-style-type: none"> • Lose the accuracy of the accessible solar irradiation.
Windows area is not accounted for in the simulated module.	<ul style="list-style-type: none"> • Helps to find the most optimal grids in the building. • Maximising the harvested solar irradiation. • Resulting in higher energy production. 	<ul style="list-style-type: none"> • Lose the accuracy of optimising the BIPV panels on the facade surfaces. • Make it challenging to delineate the reduction of the energy production.
Accuracy of the climate data used for the simulation.	<ul style="list-style-type: none"> • Does not consider the variation of the climate criteria, which varies from year to year. • Does not account for the reduction of the POA irradiance due to the snow accumulation on the roof surfaces. 	<ul style="list-style-type: none"> • Affect the accuracy of the simulation results • Affect the accuracy of energy generation.

Several limitations and simplifications were adopted in the methodology to facilitate designing the 3D model in Rhinoceros and conducting solar simulation. First the dimensions of the building are estimated, derived from one of the existing edifices earmarked for relocating of the building, to facilitate designing the 3D model. Therefore, this estimation is not a good representative of the exact solar incidence, as it might be in the real scenario. Moreover, this variation will affect the accuracy of the solar irradiation accessibility on the building envelop.

Another assumption is that, when modelling the 3D building in Rhinoceros, it does not account for the shadowing from the surrounding buildings. Hereof, the shadowing from the surrounding buildings will negatively affect the solar incidence on the building envelope, resulting in a reduction in the potential energy production. Finally, the 3D model of the building is designed, in Rhinoceros, as a building envelope without accounting the opening for windows in the design. Therefore, the simulation results of the solar irradiation performance will vary from the real case scenario, as the facade surfaces have a reduced area due to windows opening.

As for the conducted simulation in Grasshopper, the following limitations can be listed. The base climate data for this simulation miss, to some extent, the accuracy as it gives the average registered climate data over fifteen years [2007- 2021]. This inaccuracy makes it very challenging to determine the exact solar irradiation incidence during the simulated periods, due to the yearly variation of the climate condition. Another limitation is that the simulation in Grasshopper does not account the snow accumulation on the roof surfaces, which gives a reduction of the solar irradiation accessibility for the roof surface and results a reduction in the energy production during this period. Finally, the simulation does not calculate the additional solar irradiation accessibility reflected from the snow (albedo effect) on the facade surfaces.

4. Conclusion

The results from the calculations indicate that power production during the winter months is considerably lower than in the summer months. Additionally, the angle of the roof and the inclusion of panels on the facades significantly impact the overall production value, particularly during the months when the sun is positioned at a lower angle. While in theory, the total production value could cover the energy consumption of an average household, the practicality of this scenario is limited. The higher energy consumption during colder months coincides with lower production values, making it necessary to store electricity generated during summer. However, current technology is not a viable option, as it would require expensive and large-scale batteries to store enough energy that could cover the winter energy consumption.

Furthermore, commercially available BIPV modules that comply with the cultural heritage requirements regarding colour and design are limited and offer relatively low electrical efficiency. In comparison, commercially available PV solar cells' electrical efficiency must be improved to maximise energy production from harvested solar irradiation. Consequently, it is unrealistic to expect complete coverage of energy demand during seasons with fewer sun hours and lower radiation.

Several aspects were not considered during the simulation, such as potential shadows cast by surrounding buildings, trees, or other structures. Furthermore, the simulations should have considered windows and doors, and there may be some inaccuracies in the climate data used. While this means that the simulated production values are slightly higher than expected, they still clearly indicate the most optimal rotation and surfaces for BIPV. Enhancing the benefits of BIPV requires advancements in both efficiency and energy storage capabilities. Further research is needed to increase the efficiency of coloured BIPVs for facades and develop smaller batteries capable of storing electricity over extended periods.

In conclusion, the benefits of implementing BIPV on the houses in Brekstadbukta are significant, and it is recommended that Ørland municipality invests in this technology. While the maximum production varies depending on the building's orientation, it is generally most advantageous to have the most prominent surfaces facing south, such as the backside of a building, with steeper slopes yielding better results. Although specific details, such as shadows from the surrounding environment and the accuracy of climate data, were not accounted for, the simulation provides a robust representation of the optimal placement and orientation for solar power production. Despite the limited sunlight hours and lower sun position during winter, the production value is high enough to result in cost savings for the residential area on their electrical bills. Furthermore, Ørland municipality will contribute to reducing Norway's carbon footprint. As technology continues to evolve, future advancements in smaller batteries with higher storage capacities and improved BIPV efficiency will enable residential areas like Brekstadbukta to become fully self-sufficient in electricity.

Acknowledgements

This work has been supported by the municipality of Ørland, Norway, and their representative Thomas Engen

References

- [1] IEA, Renewables 2021, IEA. (2021). <https://www.iea.org/reports/renewables-2021> (accessed May 20, 2023).
- [2] SolarPower Europe, SolarPower Europe feedback on the amendment of the renewable energy directive, russels, Belgium, 2021.
https://api.solarpowereurope.org/uploads/Solar_Power_Europe_REDIII_Proposal_Feedback_150e179702.pdf.
- [3] H. Gholami, H. Nils Røstvik, K. Steemers, The contribution of Building-Integrated Photovoltaics (BIPV) to the concept of nearly zero-energy cities in Europe: Potential and challenges ahead, *Energies* (Basel). 14 (2021) 6015. <https://doi.org/10.3390/en14196015>.
- [4] A.K. Shukla, K. Sudhakar, P. Baredar, Recent advancement in BIPV product technologies: A review, *Energy Build.* 140 (2017) 188–195. <https://doi.org/10.1016/J.ENBUILD.2017.02.015>.
- [5] H. Gholami, H. Nils Røstvik, N. Manoj Kumar, S.S. Chopra, Lifecycle cost analysis (LCCA) of tailor-made building integrated photovoltaics (BIPV) façade: Solsmaragden case study in Norway, *Solar Energy.* 211 (2020) 488–502. <https://doi.org/10.1016/J.SOLENER.2020.09.087>.
- [6] P.-O.A. Borrebæk, B.P. Jelle, Z. Zhang, Avoiding snow and ice accretion on building integrated photovoltaics – challenges, strategies, and opportunities, *Solar Energy Materials and Solar Cells.* 206 (2020) 110306. <https://doi.org/10.1016/J.SOLMAT.2019.110306>.
- [7] P.-O. Andersson, B.P. Jelle, Z. Zhang, Passive snow repulsion: A state-of-the-art review illuminating research gaps and possibilities, *Energy Procedia.* 132 (2017) 423–428. <https://doi.org/10.1016/J.EGYPRO.2017.09.650>.
- [8] Ministry of Climate and Environment, Act concerning the cultural heritage, LovData, 1978. <https://lovdata.no/dokument/NLE/lov/1978-06-09-50> (accessed May 20, 2023).
- [9] Weather Spark, Climate and average weather year round in Brekstad, Weather Spark. (2023). <https://weatherspark.com/y/65516/Average-Weather-in-Brekstad-Norway-Year-Round> (accessed May 20, 2023).
- [10] Forme Solar, How wind affects solar panels?, Forme Solar,. (n.d.). <https://formesolar.com/how-wind-affects-solar-panels/> (accessed May 20, 2023).
- [11] M.J.R. Perez, V. Fthenakis, A lifecycle assessment of façade BIPV in New York, in: 37th IEEE Photovoltaic Specialists Conference, IEEE, Seattle, WA, USA, 2011: pp. 003271–003276. <https://doi.org/10.1109/PVSC.2011.6186636>.
- [12] Sun direction, Sun direction in Brekstad (Norway), Sun Direction. (2023). <https://sun-direction.com/city/44762,brekstad/> (accessed May 20, 2023).

- [13] R.S. Kamel, A.S. Fung, Modeling, simulation and feasibility analysis of residential BIPV/T+ASHP system in cold climate - Canada, *Energy Build.* 82 (2014) 758–770. <https://doi.org/10.1016/J.ENBUILD.2014.07.081>.
- [14] B.P. Jelle, T. Gao, S.A. Mofid, T. Kolås, P.M. Stenstad, S. Ng, Avoiding snow and ice formation on exterior solar cell surfaces – A review of research pathways and opportunities, *Procedia Eng.* 145 (2016) 699–706. <https://doi.org/10.1016/J.PROENG.2016.04.084>.
- [15] R.M.& Associates, Rhinoceros 3D, version 7.28, (2022). <https://www.rhino3d.com/>.
- [16] M. Formolli, T. Kleiven, G. Lobaccaro, Solar accessibility at the neighborhood scale: A multi-domain analysis to assess the impact of urban densification in Nordic built environments, *Solar Energy Advances.* 2 (2022) 100023. <https://doi.org/10.1016/J.SEJA.2022.100023>.
- [17] J. de S. Freitas, J. Cronemberger, R.M. Soares, C.N.D. Amorim, Modeling and assessing BIPV envelopes using parametric Rhinoceros plugins Grasshopper and Ladybug, *Renew Energy.* 160 (2020) 1468–1479. <https://doi.org/10.1016/J.RENENE.2020.05.137>.
- [18] M.S. Roudsari, M. Pak, LADYBUG: A parametric environmental plugin for grasshopper to help designers create an environmentally-conscious design, in: 13th Conference of International Building Performance Simulation Association, Chambéry, France, 2013. <https://www.aivc.org/resource/ladybug-parametric-environmental-plugin-grasshopper-help-designers-create-environmentally> (accessed May 20, 2023).
- [19] G. Peronato, J.H. Kämpf, E. Rey, M. Andersen, Integrating urban energy simulation in a parametric environment: a Grasshopper interface for CitySim, PLEA 2017 Edinburgh - Design to Thrive - Volume II. (2017). <https://infoscience.epfl.ch/record/228832> (accessed May 20, 2023).
- [20] Climate One Building, Repository of free climate data for building performance simulation, Climate One Building. (2023). <https://www.climate.onebuilding.org/> (accessed May 20, 2023).
- [21] A. Røyset, T. Kolås, B.P. Jelle, Coloured building integrated photovoltaics: Influence on energy efficiency, *Energy Build.* 208 (2020) 109623. <https://doi.org/10.1016/J.ENBUILD.2019.109623>.
- [22] M. Manni, M.C. Failla, A. Nocente, G. Lobaccaro, B.P. Jelle, The influence of icephobic nanomaterial coatings on solar cell panels at high latitudes, *Solar Energy.* 248 (2022) 76–87. <https://doi.org/10.1016/J.SOLENER.2022.11.005>.
- [23] L. Maturi, G. Belluardo, D. Moser, M. Del Buono, BIPV system performance and efficiency drops: Overview on PV module temperature conditions of different module types, *Energy Procedia.* 48 (2014) 1311–1319. <https://doi.org/10.1016/J.EGYPRO.2014.02.148>.
- [24] K. Fredriksen, Vi bruker mindre strøm hjemme, Statistisk Sentralbyrå. (2018). <https://www.ssb.no/energi-og-industri/artikler-og-publikasjoner/vi-bruker-mindre-strom-hjemme> (accessed May 20, 2023).

Appendices

Appendix A – Winter solar energy production

Winter							
Surfaces	Optimal Orientation	Solar Irradiation			Solar Energy [J]		
		[°]	[kWh/m ² *t]	[Area*t]	18 %	16%	14%
Right Facade	A	260	122.24	3831.48	689.67	613.04	536.41
	B	250	88.97	586.34	105.54	93.81	82.09
	C	240	86.50	326.99	58.86	52.32	45.78
Left & Back Facade	F	80	122.24	3479.41	626.29	556.71	487.12
	G	100	101.62	1097.50	197.55	175.60	153.65
	I	350	128.71	6100.71	1098.13	976.11	854.10
Front Facade	L1	170	129.39	962.70	173.29	154.03	134.78
	L2	170	74.53	924.19	166.35	147.87	129.39
	L3	180	114.52	366.81	66.03	58.70	51.35
	M	160	109.69	1376.66	247.80	220.27	192.73
	N1	180	116.21	929.68	167.34	148.75	130.15
	N2	170	102.84	1170.34	210.66	187.25	163.84
Roof	D	260	106.87	1638.54	294.93	262.17	229.39
	E	90	113.05	1733.26	311.99	277.32	242.66
	H	350	107.87	7918.89	1425.40	1267.02	1108.64
	J	170	101.09	6332.63	1139.87	1013.22	886.57
	K2	190	52.07	460.47	82.88	73.68	64.47
	K3	180	65.27	119.82	21.57	19.17	16.77

Appendix B – Spring solar energy production

		Spring					
<i>Surfaces</i>	<i>Best Orientation</i>	<i>Radiation</i>		<i>Efficiency</i>			
<i>[-]</i>	<i>[°]</i>	<i>[kWh/m²*t]</i>	<i>[Area*t]</i>	<i>18 %</i>	<i>16%</i>	<i>14%</i>	
Right Facade	A	230	323.40	10136.04	1824.49	1621.77	1419.05
	B	200	238.71	1573.09	283.16	251.69	220.23
	C	290	235.64	890.73	160.33	142.52	124.70
Left & Back Facade	F	50	323.40	9204.66	1656.84	1472.75	1288.65
	G	70	274.73	2967.12	534.08	474.74	415.40
	I	340	363.65	17236.91	3102.64	2757.91	2413.17
Front Facade	L1	170	373.91	2781.88	500.74	445.10	389.46
	L2	210	209.96	2603.47	468.62	416.55	364.49
	L3	170	277.92	890.04	160.21	142.41	124.61
	M	160	274.47	3444.64	620.04	551.14	482.25
	N1	180	268.67	2149.39	386.89	343.90	300.91
	N2	120	312.91	3560.87	640.96	569.74	498.52
Roof	D	260	471.14	7223.39	1300.21	1155.74	1011.28
	E	80	478.88	7342.04	1321.57	1174.73	1027.89
	H	350	491.51	36083.30	6494.99	5773.33	5051.66
	J	170	474.81	29743.55	5353.84	4758.97	4164.10
	K2	160	334.15	2954.68	531.84	472.75	413.66
	K3	210	382.23	701.64	126.29	112.26	98.23

Appendix C – Summer solar energy production

		Summer					
<i>Surfaces</i>	<i>Best Orientation</i>	<i>Radiation</i>		<i>Efficiency</i>			
<i>[-]</i>	<i>[°]</i>	<i>[kWh/m²*t]</i>	<i>[Area*t]</i>	<i>18 %</i>	<i>16%</i>	<i>14%</i>	
Right Facade	A	230	312.09	9781.72	1760.71	1565.07	1369.44
	B	200	230.01	1515.76	272.84	242.52	212.21
	C	290	220.92	835.09	150.32	133.61	116.91
Left & Back Facade	F	50	312.09	8882.89	1598.92	1421.26	1243.61
	G	70	264.93	2861.26	515.03	457.80	400.58
	I	340	349.46	16564.60	2981.63	2650.34	2319.04
Front Facade	L1	160	359.14	2672.02	480.96	427.52	374.08
	L2	160	201.12	2493.89	448.90	399.02	349.14
	L3	120	267.81	857.67	154.38	137.23	120.07
	M	100	265.04	3326.22	598.72	532.20	465.67
	N1	140	302.00	2415.98	434.88	386.56	338.24
	N2	130	259.22	2949.90	530.98	471.98	412.99
Roof	D	260	448.79	6880.83	1238.55	1100.93	963.32
	E	70	456.39	6997.27	1259.51	1119.56	979.62
	H	350	468.45	34390.77	6190.34	5502.52	4814.71
	J	170	449.01	28127.72	5062.99	4500.43	3937.88
	K2	230	315.75	2791.98	502.56	446.72	390.88
	K3	170	362.80	665.96	119.87	106.55	93.23

Appendix D - Autumn solar energy production

		Autumn					
<i>Surfaces</i>	<i>Best Orientation</i>	<i>Radiation</i>		<i>Efficiency</i>			
<i>[-]</i>	<i>[°]</i>	<i>[kWh/m²*t]</i>	<i>[Area*t]</i>	<i>18%</i>	<i>16%</i>	<i>14%</i>	
Right Facade	A	260	109.06	3418.24	615.28	546.92	478.55
	B	250	81.94	540.00	97.20	86.40	75.60
	C	240	78.80	297.86	53.61	47.66	41.70
Left & Back Facade	F	80	109.06	3104.14	558.75	496.66	434.58
	G	110	91.29	985.96	177.47	157.75	138.03
	I	350	114.27	5416.30	974.93	866.61	758.28
Front Facade	L1	170	114.94	855.12	153.92	136.82	119.72
	L2	170	66.56	825.40	148.57	132.06	115.56
	L3	180	103.19	330.46	59.48	52.87	46.26
	M	170	99.18	1244.75	224.05	199.16	174.26
	N1	180	103.27	826.20	148.72	132.19	115.67
	N2	170	92.47	1052.36	189.43	168.38	147.33
Roof	D	260	95.41	1462.81	263.31	234.05	204.79
	E	90	100.15	1535.43	276.38	245.67	214.96
	H	350	95.55	7014.54	1262.62	1122.33	982.04
	J	170	90.52	5670.47	1020.68	907.27	793.87
	K2	190	45.86	405.51	72.99	64.88	56.77
	K3	180	57.41	105.39	18.97	16.86	14.75